



# Early Detection and Investigation of Extracellular Vesicles Biomarkers in Breast Cancer

Erika Bandini<sup>1\*</sup>, Tania Rossi<sup>1</sup>, Emanuela Scarpì<sup>2</sup>, Giulia Gallerani<sup>1</sup>, Ivan Vannini<sup>1</sup>, Samanta Salvi<sup>1</sup>, Irene Azzali<sup>2</sup>, Mattia Melloni<sup>1</sup>, Sara Salucci<sup>3</sup>, Michela Battistelli<sup>4</sup>, Patrizia Serra<sup>2</sup>, Roberta Maltoni<sup>5</sup>, William C. Cho<sup>6</sup> and Francesco Fabbri<sup>1</sup>

<sup>1</sup>Biosciences Laboratory, IRCCS Istituto Romagnolo per Lo Studio Dei Tumori (IRST) "Dino Amadori", Meldola, Italy, <sup>2</sup>Biostatistics and Clinical Trials Unit, IRCCS Istituto Romagnolo per Lo Studio Dei Tumori (IRST) "Dino Amadori", Meldola, Italy, <sup>3</sup>Cellular Signalling Laboratory, Department of Biomedical and NeuroMotor Sciences (DIBINEM), University of Bologna, Bologna, Italy, <sup>4</sup>Department of Biomolecular Sciences, University of Urbino Carlo Bo, Urbino, Italy, <sup>5</sup>Department of Medical Oncology, IRCCS Istituto Romagnolo per Lo Studio Dei Tumori (IRST) "Dino Amadori", Meldola, Italy, <sup>6</sup>Department of Clinical Oncology, Queen Elizabeth Hospital, Kowloon, Hong Kong, China

## OPEN ACCESS

### Edited by:

Jian-ye Zhang,  
Guangzhou Medical University, China

### Reviewed by:

Paschalia Pantazi,  
Imperial College London,  
United Kingdom  
Célio Junior da Costa Fernandes,  
São Paulo Research Foundation  
(FAPESP), Brazil

### \*Correspondence:

Erika Bandini  
erika.bandini@irst.emr.it

### Specialty section:

This article was submitted to  
Cellular Biochemistry,  
a section of the journal  
Frontiers in Molecular Biosciences

**Received:** 29 June 2021

**Accepted:** 07 September 2021

**Published:** 08 November 2021

### Citation:

Bandini E, Rossi T, Scarpì E, Gallerani G, Vannini I, Salvi S, Azzali I, Melloni M, Salucci S, Battistelli M, Serra P, Maltoni R, Cho WC and Fabbri F (2021) Early Detection and Investigation of Extracellular Vesicles Biomarkers in Breast Cancer. *Front. Mol. Biosci.* 8:732900. doi: 10.3389/fmolb.2021.732900

Breast cancer (BC) is the most commonly diagnosed malignant tumor in women worldwide, and the leading cause of cancer death in the female population. The percentage of patients experiencing poor prognosis along with the risk of developing metastasis remains high, also affecting the resistance to current main therapies. Cancer progression and metastatic development are no longer due entirely to their intrinsic characteristics, but also regulated by signals derived from cells of the tumor microenvironment. Extracellular vesicles (EVs) packed with DNA, RNA, and proteins, are the most attractive targets for both diagnostic and therapeutic applications, and represent a decisive challenge as liquid biopsy-based markers. Here we performed a study based on a multiplexed phenotyping flow cytometric approach to characterize BC-derived EVs from BC patients and cell lines, through the detection of multiple antigens. Our data reveal the expression of EVs-related biomarkers derived from BC patient plasma and cell line supernatants, suggesting that EVs could be exploited for characterizing and monitoring disease progression.

**Keywords:** breast cancer, extracellular vesicles, plasma, liquid biopsy, biomarkers

## INTRODUCTION

Breast cancer (BC) is the most commonly diagnosed malignant tumor in women worldwide, and the leading cause of cancer death in the female population. Although it has been calculated that in Europe, between 2014 and 2019, cancer mortality rate has declined steadily by about 8.7% (Malvezzi et al., 2019), an incidence of 2,261,419 cases and 684,996 deaths were reported

in 2020, remaining an alarming concern for public health (Sung et al., 2021). In fact, despite improved clinical management resulting in better prognosis, up to 30% of node-negative BC patients and a larger part of patients with node-positive carcinoma, develop distant metastases after several years from the time of primary tumor detection and surgical resection (Barone et al., 2020). This provides only a relatively poor chance for successful treatments and survival, and identification of new molecular markers for diagnosis and prognosis, especially in a metastatic setting, and for development of innovative therapeutic molecules, are necessary. Furthermore, BC is characterized by a considerable tissue heterogeneity, showing distinct clinical and biological features, which make tumors respond differently to treatments and adverse in their management. In the last years, molecular profiles have been largely explored, providing a well-established classification of BCs into four well-settled subtypes: Luminal A, Luminal B, Basal-like, and human epidermal growth factor receptor 2 (Her2)-enriched. In addition, BC staging also provides useful information about appropriate treatment options, due to its ability to estimate prognosis at each tumor stage. In particular, the Tumor-Node-Metastasis (TNM) system represents an attempt to classify cancer based on the major morphological attributes of malignant tumors that were thought to influence disease prognosis: size of the primary tumor (T), presence and extent of regional lymph node involvement (N), and presence of distant metastases (M) (Singletary and Connolly, 2006; Bandini and Fanini, 2019).

Neovascularization has become a pivotal aspect of tumor and metastasis growth, involving endothelial cell (EC) proliferation, migration, and vascular formation (Chen et al., 2019). In the last years, research has narrowed its attention to the study of the tumor microenvironment (TME) as a target for cancer therapy. In fact, chemoresistance of tumor cells and the development of metastases are no longer due entirely to their intrinsic characteristics, but are also regulated by signals derived from cells of TME. Secreted factors from cancerous cells enable the recruitment of several types of cells required to form the TME, contributing to the formation of a premetastatic niche and to development of chemoresistance (Madden et al., 2020). Tumor stromal cells, including fibroblasts, immunoinflammatory cells, vascular EC and other components of TME, as well as the extracellular matrix, not only play a crucial role in cancer response to therapies, but also orchestrate cancer proliferation, invasion, and metastasis. In particular, ECs are the building pillars of vessels and as such are key players in sprouting angiogenesis (Draoui et al., 2017). Recently, several models and analysis tools have been developed to investigate the crosstalk between mammary cells and neighboring vascular ECs, in order to explore their potential applications in basic research and drugs development. In fact, it could be useful to establish new approaches to develop anti-angiogenic strategies, which represent the few available

therapies against the most aggressive BCs (Devadas et al., 2019; Kourti et al., 2020).

Since most of the current methods used for diagnosis and prognosis of cancer are expensive, invasive, and time consuming, new diagnostic panels need to be investigated to make the process less invasive, more cost-effective, and rapid. Among the most promising potential diagnostic targets, extracellular vesicles (EVs) are nanometer-sized, lipid membrane-enclosed vesicles released by many types of cells and classified by different size, components, and functions (Xue et al., 2021). EVs are normally distinguished into three main classes: microvesicles produced through outward budding and fission of the plasma membrane, exosomes derived from endosomes and fusion of multivesicular bodies with the plasma membrane, and apoptotic bodies released as blebs from apoptosis undergoing cells (Wu et al., 2019). Importantly, EVs are the most attractive targets for both therapeutic and diagnostic applications, especially because they are enriched in a large batch of body fluids such as breast milk (Shah et al., 2021), blood plasma (Hu H. et al., 2021), saliva (Hoshino, 2021), urine, serum (Salvi et al., 2021), and cerebrospinal fluid (López-Pérez et al., 2021), becoming an excellent source of potential biomarkers. All cell types are expected to secrete EVs, but their main functions remain to be fully understood. In particular, exosomes are membrane-bound vesicles, 50–200 nm in size, secreted from cells *via* a multivesicular-body endocytic process. This vesicles population has been proposed to perform main functions, among which they are counted to support processes to eliminate DNA, RNA, or protein content that could be detrimental to cell viability, to maintain a cell-to-cell communication system by delivering cargo to a recipient cell, or even to develop a mechanism for surveying cell content for viral infections (Sempere et al., 2017; Jayaseelan, 2020). EVs are enriched in proteins involved in the vesicles' trafficking, cell surface receptors such as tumor susceptibility gene 101 (TSG101), integrins and a number of tetraspanins such as CD9, CD53, CD63, CD81, and CD82 (Burgio et al., 2020). The study of exosomes is relatively difficult and, as referred by the International Society of Extracellular Vesicles (ISEV), the assignment of a specific biogenesis pathway to EVs remains not easy to establish as it could be validated only through a live imaging assay of EV release. Accordingly, due to current technical limitations, almost all studies are unable to isolate and investigate a pure population of exosomes (Romano et al., 2021). Despite being a validated source of biomarkers, liquid biopsy (LB) has not yet succeeded in becoming part of the standard clinical practice in BC patients (Chan et al., 2021). The deepening of isolation and analysis of EVs is essential for understanding their biological roles and for investigating their potential clinical use. Several methods have been developed thus far, but with some limitations (Jong et al., 2017).

The present work aimed at identifying new BC tumor biomarkers through an easy and fast approach, based on a

multiplexed phenotyping of EVs released from 30 plasma samples of 10 BC patients. Second, results obtained from patients revealed adhesion molecules markers usually present on the surface of circulating endothelial cells, prompting us to investigate also cell models. Through the analysis of supernatant of BC cell lines, cultured alone or with ECs, we aspired to find clues regarding: 1) EV origin subtypes comparing biomarkers found in plasma and in BC cell cultures and 2) cancer-normal cell interplay, detecting potential marker expression changes in co-culture conditions. EVs were isolated by size exclusion chromatography (SEC) and characterized by a bead-based cytofluorimetric method able to simultaneously detect 37 surface exosomal-related proteins.

## MATERIALS AND METHODS

### Cell Cultures

The human breast carcinoma cell lines, MDA-MB 453 (Her2-enriched subtype) and MCF-7 (Luminal A molecular subtype) were purchased from ATCC (ATCC; Manassas, Virginia, United States), and cell lines T-47D (Luminal A molecular subtype) and HUVEC (Normal Primary Human Umbilical Vein Endothelial Cells) were purchased from zooprophyllactic Institute of Genova (Italy). MDA-MB 453 were maintained in Leibovitz's L-15 medium (ATCC 30-2008, United States). MCF-7 were maintained in EMEM medium (ATCC 30-2003). T47D were maintained in DMEM High Glucose (Euroclone, Italy). HUVEC were maintained in M199 medium (Sigma Aldrich, Merck, Germany). Each medium was supplemented with FBS exosome-depleted (Gibco, Thermo Fisher Scientific, United States) to a final concentration of 10%, according to the information sheet of the manufacturer. Penicillin-streptomycin (PAA, Carlo Erba Reagents, Italy) to a final concentration of 1% and MycoZap Prophylactic (Lonza Group Ltd., Switzerland) to a final concentration of 0.002% were added to all media. The cultures were maintained in an incubator Heraeus, in an atmosphere composed of 95% air and 5% CO<sub>2</sub>, except for MDA-MB-453 that required a free gas exchange with atmospheric air. Every 4 days we proceeded to the sub-cultivation of cell lines

by using Trypsin-EDTA (Life Technologies, United States). Cell lines were tested every 2 months with MycoAlert™ *Mycoplasma* Detection Kit (Lonza Group Ltd., Switzerland) to check a possible contamination by *mycoplasma*.

### Patient Sample Collection

The study was conducted on 21 individuals: 10 BC patients diagnosed with early-stage BC enrolled between 2013 and 2014, as well as 11 healthy donors. The samples were enrolled at the Istituto Scientifico Romagnolo per lo Studio e la Cura dei Tumori IRST. Peripheral whole blood was collected at three time points: 1 day before surgery (A), 1 month after surgery (B), and after adjuvant therapy/6 months after surgery (C). None of the patients underwent neoadjuvant therapy or had detectable metastasis at diagnosis. Histological and clinical characteristics are listed in **Table 1**. Written informed consent was obtained from all subjects before sample analyses. The study was approved by the Ethical Committee of our Institute, Romagna Ethics Committee (CEROM) of Meldola (IRSTB008) and conducted in accordance with the Declaration of Helsinki. Healthy donors were enrolled at the Istituto Scientifico Romagnolo per lo Studio e la Cura dei Tumori IRST and were matched to BC patients for age classes (all female with an average age of 55).

### Plasma and Supernatant Collection

Approximately 5 mL of whole blood were collected in EDTA tubes and centrifuged at 1,000 × g for 15 min, followed by a second centrifugation at 1,500 × g 10 min for obtaining plasma. The blood was collected from all individuals before any surgical intervention, 1 month after surgery and after adjuvant therapy/6 months after surgery. Plasma samples were conserved at -80°C until use. Approximately 30 ml of supernatant of BC controls and co-cultured cells were collected 48 h post co-culture and immediately processed to isolate EVs.

### Co-Culture Experiments

Transwell Permeable Supports (Corning, United States) with a 0.45 μm polycarbonate membrane were used in the co-culture model system to separate BC and HUVEC cells

**TABLE 1** | Clinical pathological characteristics of patients. Tumor stage was reported based on the tumor (T), lymph node (N), and metastasis (M) system.

| Patient | Age | Subtype | Histology         | T  | N (positive/asported) | M | Grade | Vascular invasion |
|---------|-----|---------|-------------------|----|-----------------------|---|-------|-------------------|
| 1       | 57  | TNBC    | Ductal infiltrant | 2  | 0 (1)                 | 0 | 3     | Yes               |
| 2       | 75  | LumA    | Ductal infiltrant | 1b | 0 (2)                 | 0 | 2     | No                |
| 3       | 43  | TNBC    | Ductal infiltrant | 1c | 1a (1/35)             | 0 | 3     | No                |
| 4       | 58  | TNBC    | Ductal infiltrant | 2  | 1a (2/28)             | 0 | 3     | Yes               |
| 5       | 59  | LumA    | Ductal infiltrant | 1b | 0(1)                  | X | 3     | Yes               |
| 6       | 43  | TNBC    | Ductal infiltrant | 1c | 0 (1)                 | X | 3     | No                |
| 7       | 53  | LumA    | Ductal infiltrant | 2  | 1a (1/15)             | X | 2     | Yes               |
| 8       | 57  | LumA    | Ductal infiltrant | 1b | 0 (1)                 | X | 1     | No                |
| 9       | 59  | LumA    | Lobular           | 1c | 0 (2)                 | 0 | 2     | No                |
| 10      | 54  | LumA    | Ductal infiltrant | 1c | 0 (1)                 | X | 2     | No                |

into different compartments. HUVEC cells were seeded into a six well plate (lower chamber) and an equivalent number of BC cells (ratio 1:1) were seeded into the transwell insert, which was then placed directly over the 6-well plate containing the HUVECs. BC and HUVEC controls were seeded separately into a six well plate. All cells were maintained in FBS exosome-depleted medium. Two independent experiments were performed and all the 3 cell lines were used (control groups,  $n = 3$  and co-cultured groups,  $n = 3$ ). Cells were incubated for 48 h and then washed in PBS 1X and harvested for further analysis.

## Isolation of EVs From Cell Culture Medium and Plasma of BC Patients

30–40 mL of supernatants from BC and HUVEC cells containing exosome-depleted FBS (Gibco, Thermo Fisher Scientific, United States) were collected after 48 h co-culture, centrifuged at  $300 \times g$  for 10 min, filtered by 0.22  $\mu\text{m}$  syringe to exclude cell debris and further purified by centrifugation for 15 min at  $1,000 \times g$  and for 15 min at  $2,000 \times g$ . Subsequently supernatants were concentrated through Centricon Plus-70 centrifugal filter devices (Merck Millipore, Darmstadt, Germany). For BC patients, 500  $\mu\text{L}$  of plasma were used. For EVs isolation, qEV10 Size Exclusion Columns (70 nm, Izon Science) were used. After rinsing the columns with PBS 1X, 300–500  $\mu\text{L}$  of concentrated culture medium were applied on the top of a qEV column and 0.5 mL fractions were collected. Four vesicles-enriched fractions (7–10) were firstly analyzed, then EVs content analysis was performed on fraction 8 after nanoparticle tracking analysis (NTA) evaluation.

## Nanoparticle Tracking Analysis

NTA was used to determine particles size and estimate number/ml of isolated EVs from subjects and cell lines. EVs were characterized by NTA with a NanoSight NS300 (Malvern Instruments, United Kingdom), equipped with NTA 2.3 analytical software laser. Five 30 s videos were recorded per sample in light scatter mode with a camera level of 14 and from these the software calculated the mean and the mode diameter (nm) and EV concentrations. Software settings for analysis were kept constant for all measurements. All samples were diluted in 0.1  $\mu\text{m}$  filtered PBS to an appropriate concentration before analysis. Based on the data obtained at NTA, which highlighted the fraction eight to be more concentrated and homogenous, we proceeded with downstream analyses with fraction eight for all the samples. Data were analyzed with the NTA version 2.3.

## Extraction of Proteins

Proteins were concentrated from the fraction eight of EVs obtained from plasma of patients and from supernatant of

cell lines. Then total proteins were extracted, keeping samples on ice, with 1X RIPA lysis buffer (Santa Cruz Biotechnology, United States) with the addition of 10  $\mu\text{L}$  of PMSF, 10  $\mu\text{L}$  of sodium orthovanadate and 15  $\mu\text{L}$  of protease inhibitors per ml of 1X RIPA lysis buffer, as recommended by the manufacturer's protocol. The lysates were centrifuged at  $4^\circ\text{C}$  at  $13,000 \times g$  for 30 min. Then, the supernatant was transferred to another tube. Proteins were subsequently quantified following the protocol of the BCA Protein Assay (Pierce, Thermo Fisher Scientific, United States) and using a Multiscan EX microplate reader (Thermo Fisher Scientific, United States), with a wavelength filter of 490 nm.

## Protein Expression Analyses

Western blotting was used to evaluate the expression of the exosome markers CD9, Alix, CD81, TSG-101, and Calnexin. Twenty  $\mu\text{g}$  of proteins were denatured and separated by electrophoresis using Criterion TGX Stain Free Gel Precast 4–20% (Bio-Rad Laboratories, CA, United States) and Laemmli Sample Buffer (Bio-Rad Laboratories, CA, United States) with 5% of  $\beta$ -mercaptoethanol (Carlo Erba Reagents, Italy), in 1:1 ratio with the sample. The electrophoretic run was performed at a constant voltage of 180 V in a TRIS/Glycine/SDS 1X buffer (Bio-Rad Laboratories, CA, United States). Proteins were then transferred onto a PVDF membrane (Trans-Blot Transfer Turbo midi-format 0.2  $\mu\text{m}$ ; Bio-Rad Laboratories) using the Trans Blot Turbo System (Bio-Rad Laboratories, CA, United States). The membrane was subsequently incubated for at least 2 h at room temperature in a solution of Tween 20 (Bio-Rad Laboratories, CA, United States) at 0.1% and 1X Dulbecco's Phosphate Buffered Saline (Invitrogen, Thermo Fisher Scientific, United States) supplemented with 5% milk powder (Blotting Grade Blocker Non-Fat Dry Milk; Bio-Rad) in order to facilitate the saturation of non-specific binding sites. Primary antibodies and dilutions used are the following: CD9 (D8O1A, Cell Signaling, United States) 1:1,000, Alix (3A9, Cell Signaling, United States) 1:1,000, CD81 (D4, Santa Cruz, United States) 1:1,000, TSG-101 (T5701, Sigma-Aldrich, Merck, Germany), 1:1,000 and Calnexin (2,433, Cell Signaling, United States) 1:1,000. Secondary antibodies and dilutions used are the following: Goat anti-rabbit IgG-HRP and Goat anti-mouse IgG-HRP (Santa Cruz, United States) 1:5,000, Precision Plus Protein Western C StrepTactin-HRP Conjugate (Bio-Rad Laboratories, CA, United States) 1:10,000. Blocking and immunological reactions were performed in accordance with the protocol Western Immunoblotting of Cell Signaling. Images were developed through the SuperSignal West Femto (Pierce, Thermo Fisher Scientific, United States) or Clarity West-ern ECL Substrate

(Bio-Rad Laboratories, CA, United States) and acquired through Chemidoc (Bio-Rad Laboratories, CA, United States).

## Bead-Based Multiplex Exosome Flow Cytometry Assay

Samples were subjected to bead-based multiplex EV analysis by flow cytometry (MACSPlex Exosome Kit, Miltenyi Biotec, Bergisch-Gladbach, Germany). The MACSPlex Exosome Kit (Miltenyi Biotec, Germany) allows the detection of 37 exosomal surface epitopes (CD3, CD4, CD19, CD8, HLA-DR, CD56, CD105, CD2, CD1c, CD25, CD49e, ROR1, CD209, CD9, SSEA4, HLA-BC, CD63, CD40, CD62 P, CD11c, CD81, MCSP1, CD146, CD41b, CD42a, CD24, CD86, CD44, CD326, CD133/1, CD29, CD69, CD142, CD45, CD31, CD20, and CD14) plus two isotype controls (REA and IgG1). The MACSPlex Exosome Detection Reagents for CD9, CD81, and CD63 were used to label the captured EVs. EV-containing samples were processed as follows: vesicles were diluted with MACSPlex buffer (MPB) to a final volume of 120  $\mu$ L, then 15  $\mu$ L of MACSPlex Exosome Capture Beads (containing 39 different antibody-coated bead subsets) were added to each sample. One negative/blank control (MACSPlex Buffer only) was used in each run experiment to determine non-specific signals. For counterstaining of particles bound by capture beads with detection antibodies, 5  $\mu$ L of each APC-conjugated anti-CD9, anti-CD63, and anti-CD81 detection antibody were added to each sample, then they were incubated on an orbital shaker at 450 rpm protected from light for 1 h at room temperature. Next, samples were washed with MPB and incubated on an orbital shaker at 450 rpm protected from light for 15 min. Subsequently, a further MPB washing was performed and flow cytometric analysis was carried out through a BD FACSCanto equipped with two lasers, 488 nm and 630 nm (Becton Dickinson, San Diego, CA, USA), recording a minimum of 50 events for each population of specific beads. The detection of FITC, PE, and APC fluorophores were measured for each sample. For each sample, the 39 bead populations (37 exosomal surface epitopes + 2 isotype controls) were distinguished by different fluorescence intensities detected in the FITC, PE, and APC channels. Final analysis was performed through the corresponding software (BD FACSDiva): from the raw median fluorescence intensity (MFI) of each marker was subtracted the MFI of the negative control used in the same run experiment.

## Transmission Electron Microscopy

EVs isolated from the cell lines supernatants were adsorbed to form VAR carbon coated 200 mesh grids (Agar Scientific Ltd., Stansted, United Kingdom) for 2 min, and briefly rinsed in

filtered PBS 1X. Vesicles on grids were immediately fixed with 2.5% glutaraldehyde for 1 min and then negatively stained with 2% (wt/vol) Na-phosphotungstate for 1 min. The observations were carried out by means of a Philips CM10 transmission electron microscope at 80 kV.

## Data Analysis

The images of the Western blot were acquired through Chemidoc (Bio-Rad Laboratories) and BD FACSDiva software was used to perform Flow Cytometry analysis.

## Statistical Analysis

The aim of the study was to evaluate the technical feasibility of a new workflow to investigate the potential role of EVs in early diagnosis of BC. Descriptive statistics were reported as proportions and median values (range). Non-parametric ranking test (Median test) was used to compare continuous data. MACSPlex results were analyzed by *t* test or analysis of variance (ANOVA) for repeated measures. The associations between continuous variables were determined using Spearman correlation analysis. To generate heatmaps of data, data were exported to comma separated files, which were subsequently imported into R Software for further analysis and data visualization. Mann Whitney *U* test (non-parametric ranking test) was used to compare EVs mean diameter and EVs mode diameter between healthy volunteers ( $n = 11$ ) and patients ( $n = 10$ ). Robust rank-based ANOVA (ATS) was used to detect a time effect on EVs mean diameter and EVs mode diameter in patients, and multiple comparisons (again ATS) were performed to determine which time points differed. Due to the explorative nature of the study, no formal sample size calculations were performed and no multiple test corrections were made. All *p* values were based on two-sided testing, and *p*-values  $< 0.05$  were considered statistically significant. Statistical analysis was carried out using SAS software, version 9.4 (SAS Institute, Cary, NC, United States) and R statistical package version v 4.0.0 (R Foundation for Statistical Computing, Vienna, Austria) with nparLD package version 2.1.

## RESULTS

### Characterization of EVs Isolated From Plasma

EVs were successfully isolated from plasma of BC patients and healthy donors through SEC, recently established a reliable EVs-isolation method that allows separation of EVs from a considerable portion of lipoproteins and other plasma components (Brahmer et al., 2019). NTA showed that the EVs from the plasma of BC patients had a mean size of 131.1 nm, range 95.3–151.6 nm, and a mode of 97.6. Concentrations ranged between  $4.9 \times 10^9$  –  $5.43 \times 10^{10}$  particles/ml as shown in **Figure 1**. EVs from plasma of

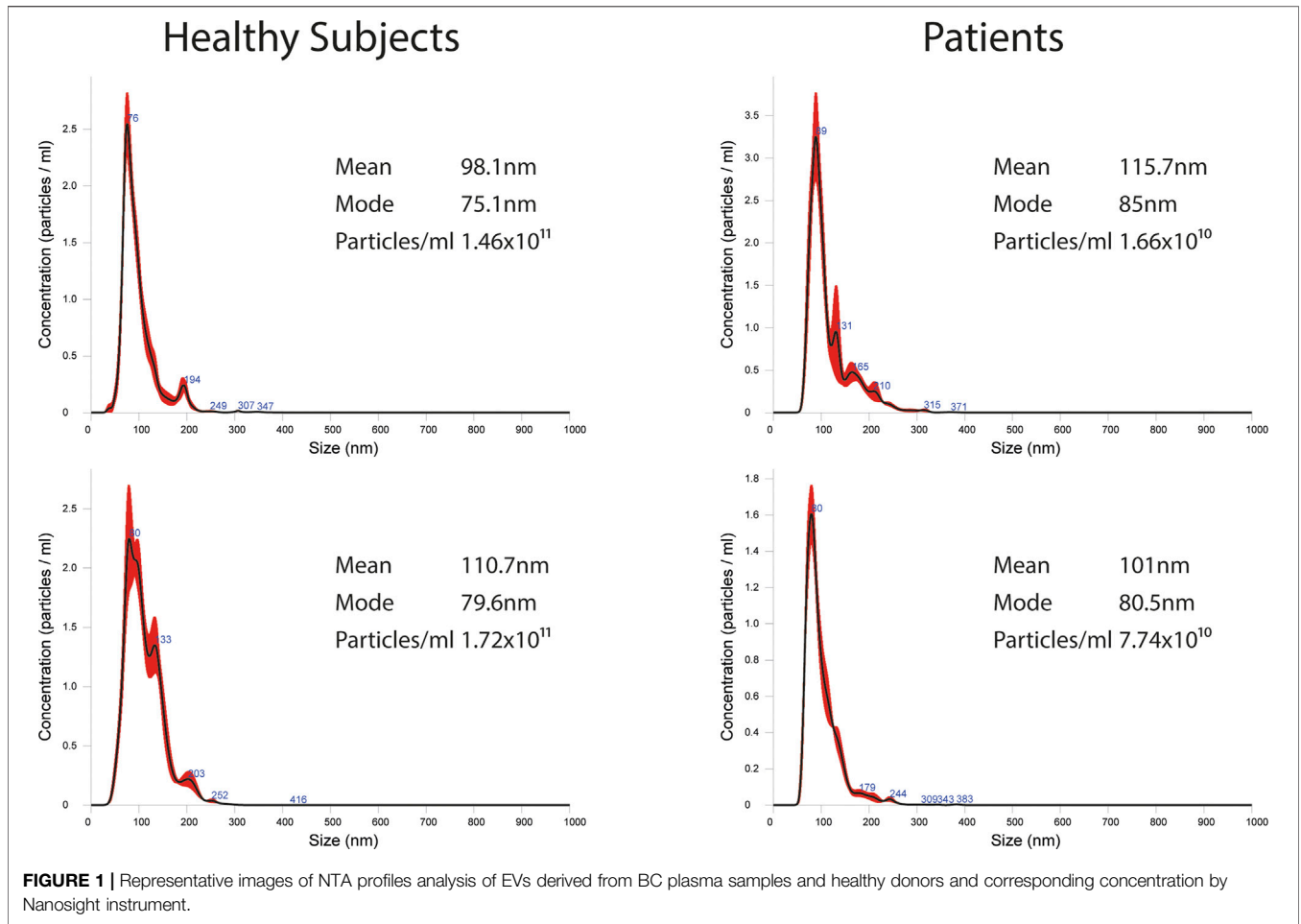


**FIGURE 1 |** Representative images of NTA profiles analysis of EVs derived from BC plasma samples and healthy donors and corresponding concentration by Nanosight instrument.

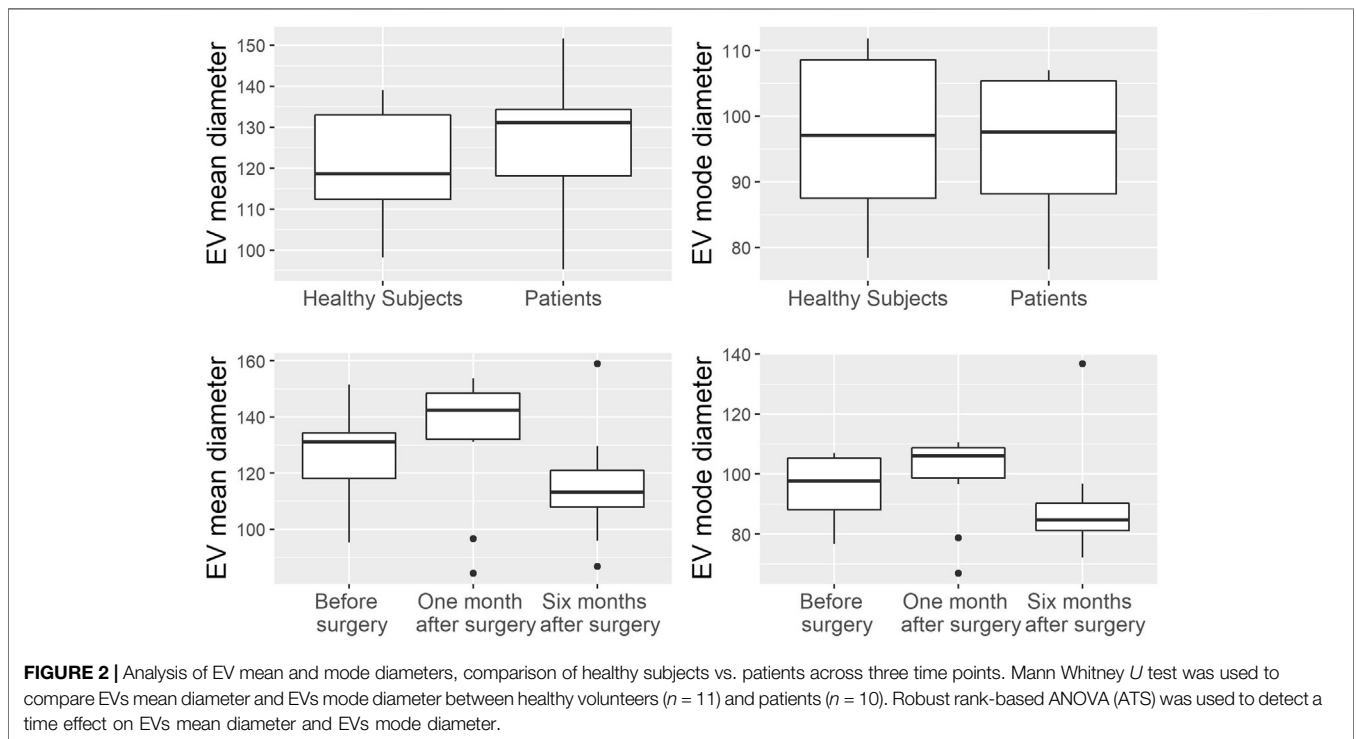
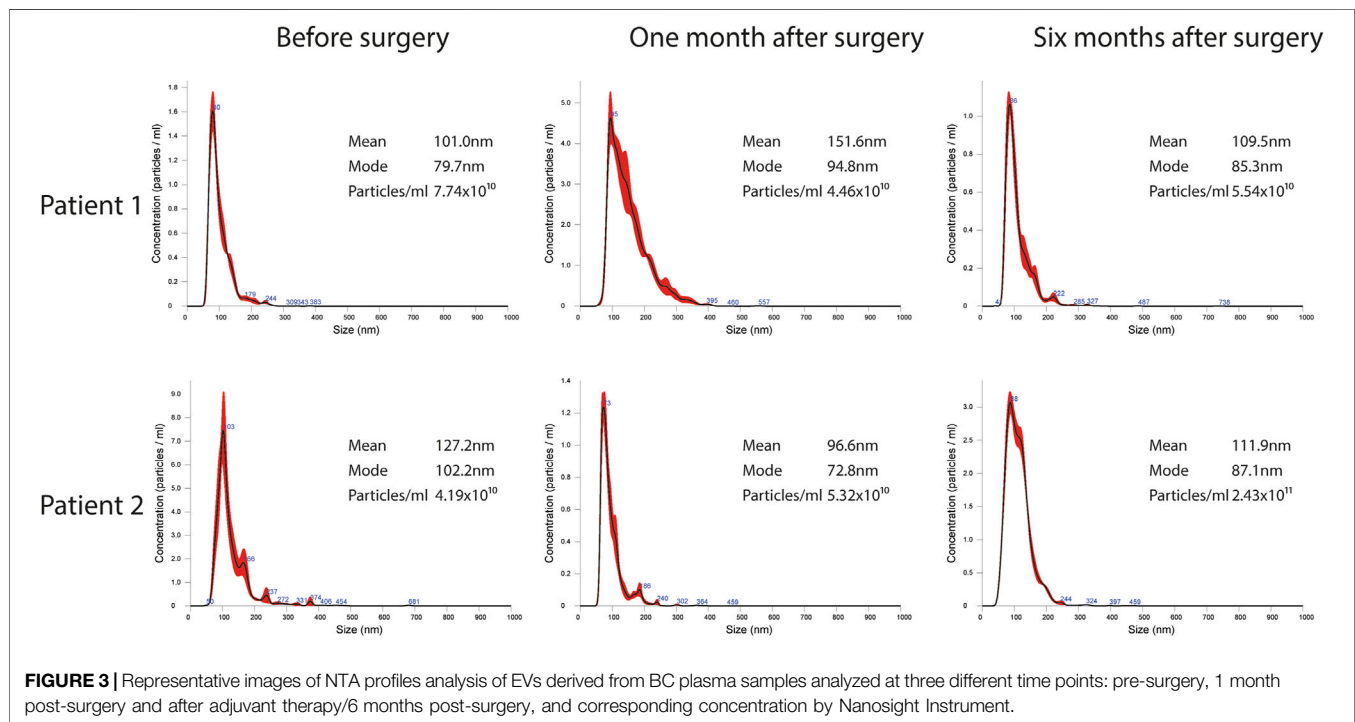
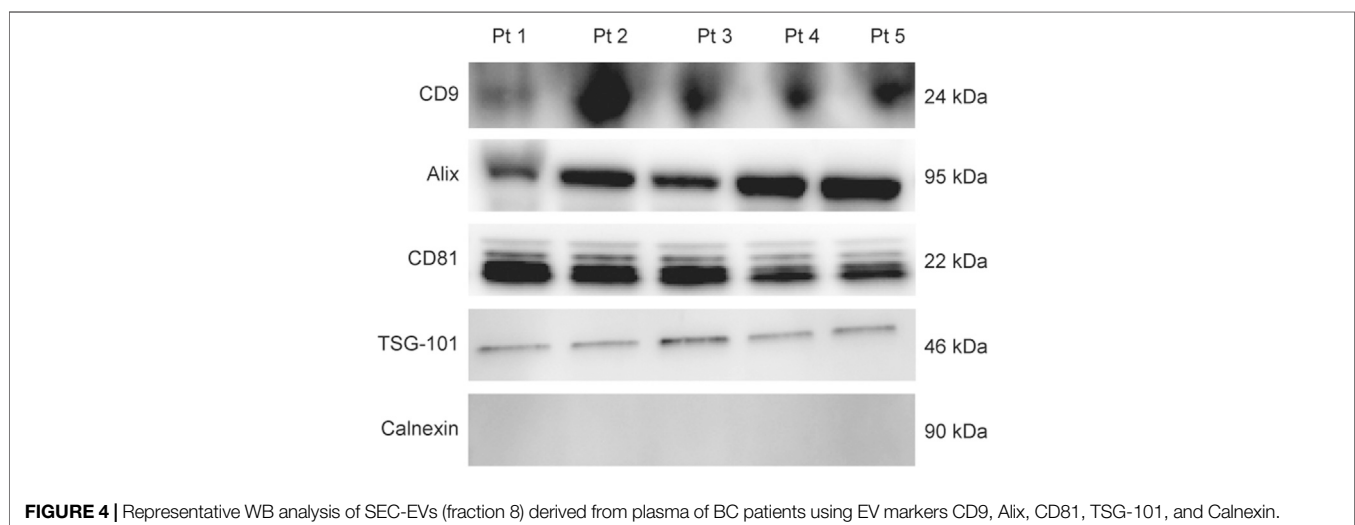


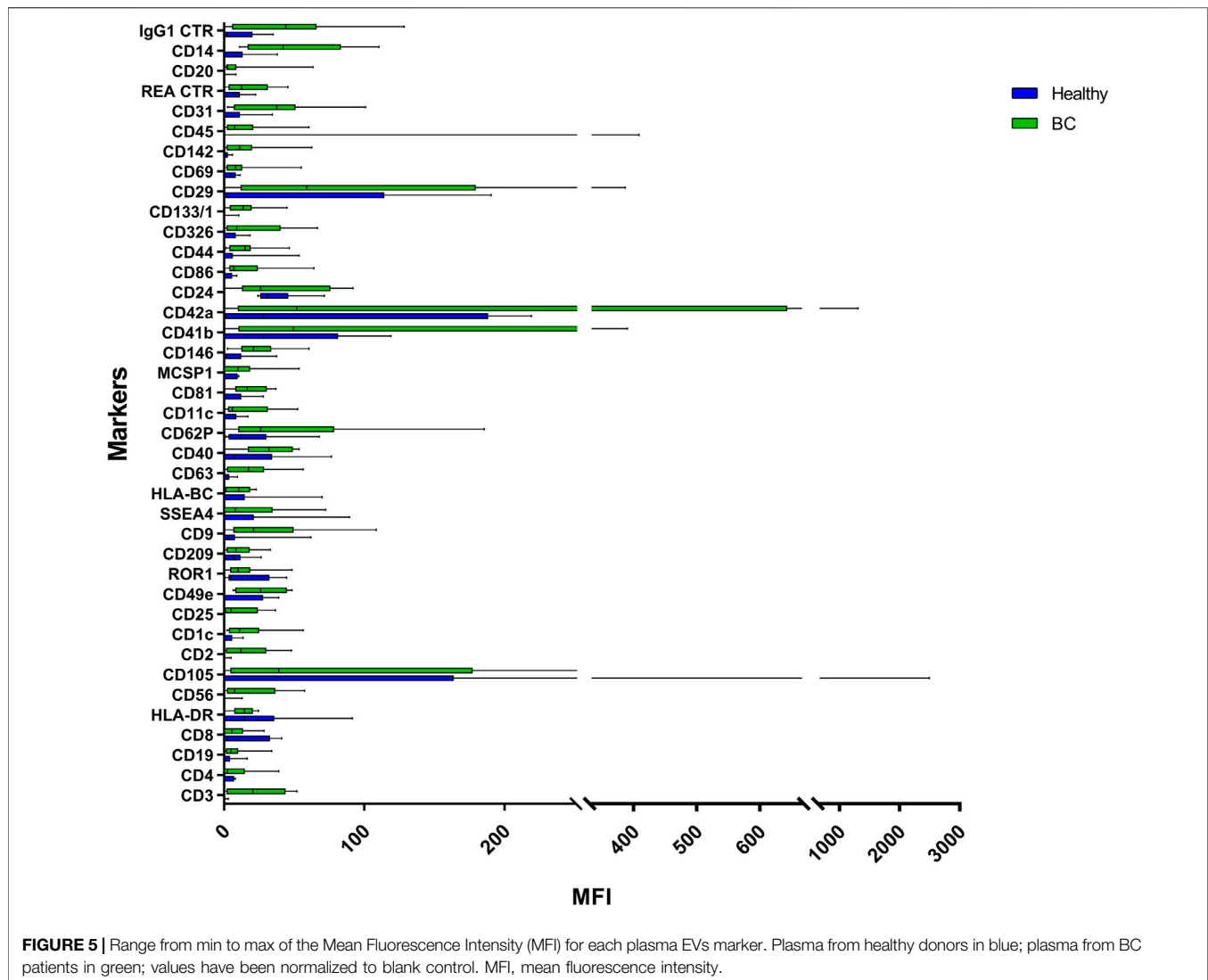
**FIGURE 2 |** Analysis of EV mean and mode diameters, comparison of healthy subjects vs. patients across three time points. Mann Whitney *U* test was used to compare EVs mean diameter and EVs mode diameter between healthy volunteers ( $n = 11$ ) and patients ( $n = 10$ ). Robust rank-based ANOVA (ATS) was used to detect a time effect on EVs mean diameter and EVs mode diameter.



healthy donors were characterized by a mean size of 118.6 nm, range 98.2–139 nm, and a mode of 97.1. No statistical difference was observed between the EV mean diameters ( $p = 0.403$ ) and the EV mode diameters ( $p = 0.802$ ) of healthy subjects vs. patients (Figure 2). Concentrations ranged between  $3.10 \times 10^9$  –  $1.72 \times 10^{11}$  particles/ml. In vesicles derived from BC patients among three time points (Figure 3), a significant time effect was detected on EV mean diameters ( $p = 0.016$ ), in particular for pre-surgery vs. post-surgery (median EV mean diameter 131.1 nm vs. 142.4 nm,  $p = 0.021$ ) and for 1 month post-surgery vs. 6 months post-surgery

(median EV mean diameter 142.4 nm vs. 113.2 nm,  $p = 0.02$ ). No significant time effect was found on EV mode diameter ( $p = 0.052$ ) (Figure 2). The isolated vesicles were analyzed for the presence of exosomal markers confirmed by western blot, showing positivity at different levels for CD9, Alix, CD81, and TSG-101 while they were negative for the expression of Calnexin (Figure 4). Furthermore, they were analyzed through flow cytometry (Figures 5, 6), revealing a variation in the expression of EVs markers between patients and healthy donors and among three different time points of BC patients.





## EV Markers Differentially Expressed in Plasma of BC Patients

Plasma EVs analysis showed that 11 significant markers were able to significantly discriminate between healthy subjects and patients: CD3, CD56, CD2, CD25, CD9, CD44, CD326, CD133/1, CD142, CD45, and CD14 (Table 2). All markers significantly distinguish healthy subjects and BC cases: CD3, CD25, CD56 ( $p < 0.001$ ); CD2, CD9, CD142, and CD14 ( $p < 0.01$ ); CD44, CD326, CD133/1, and CD45 ( $p < 0.05$ ). Statistical results confirmed the trend of tumor samples to have, on average, higher marker values than healthy ones, except for CD45 that decreases its fluorescent intensity in BC cases. Statistical differences were further observed within different time points

of BC patients for CD146 ( $p = 0.034$ ) and CD45 ( $p = 0.047$ ) (Table 3). More specifically, both markers were found downregulated 1 month after surgery compared to the first access (CD146  $p = 0.042$  and CD45  $p = 0.040$ ). Data were further evaluated by heatmap analyses, showing however only a weak clustering of CD42a and CD41b that seemed independent from subtype and time points (Supplementary Figure S1). The expression of EV markers CD105, CD1c, CD62p, CD41b, CD42a, CD326, and CD29 in BC patients was associated with age of patients (Table 4). Among them, CD1c decreased with age while the other antigens increased. In healthy subjects, only CD209 resulted inversely correlated to age, and it decreased along with the increasing of age ( $p = 0.026$ ).



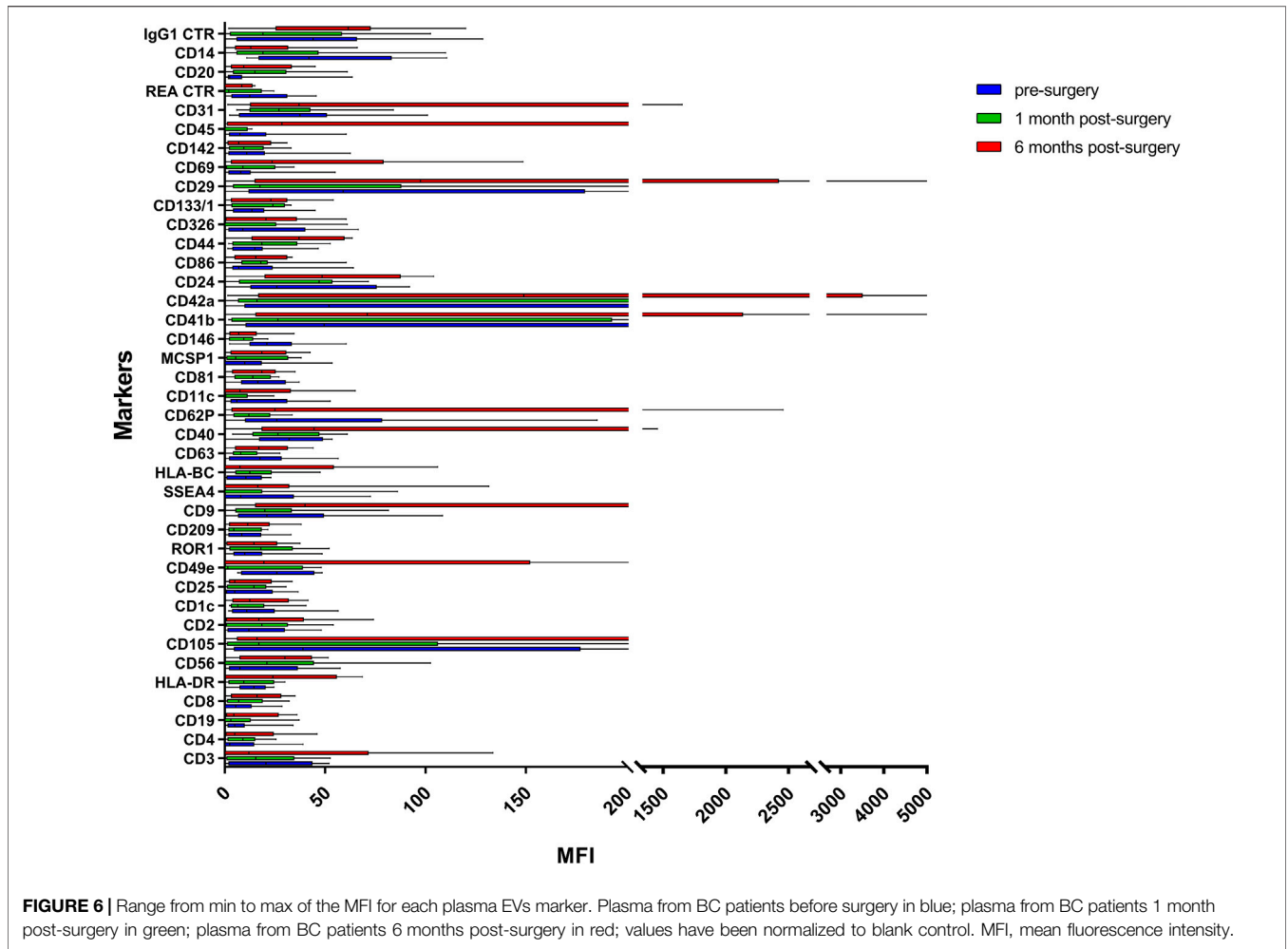


**FIGURE 6 |** Range from min to max of the MFI for each plasma EVs marker. Plasma from BC patients before surgery in blue; plasma from BC patients 1 month post-surgery in green; plasma from BC patients 6 months post-surgery in red; values have been normalized to blank control. MFI, mean fluorescence intensity.

**TABLE 2 |** Summary of significant values calculated through analysis of mean values of plasma EVs derived from healthy subjects and BC patients. MFI, mean fluorescence intensity. Unpaired Student's *t* test was used to perform analysis.

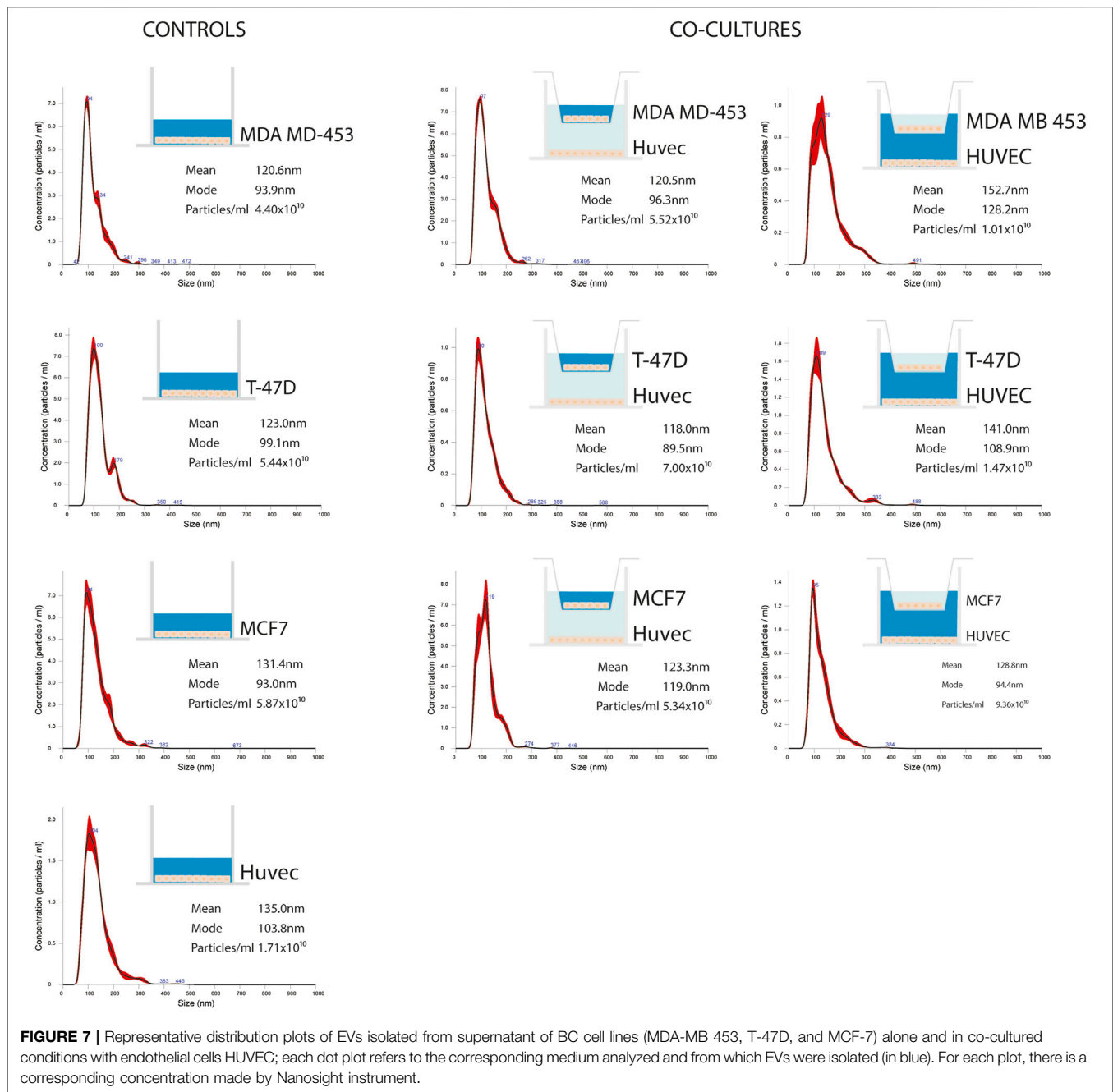
| Markers | Healthy mean MFI | BCs mean MFI | <i>p</i> -value |
|---------|------------------|--------------|-----------------|
| CD3     | 0.273            | 22.444       | 0.001           |
| CD56    | 1.182            | 17.944       | 0.001           |
| CD2     | 0.500            | 16.333       | 0.006           |
| CD25    | 0.000            | 11.444       | 0.0009          |
| CD9     | 8.455            | 33.444       | 0.006           |
| CD44    | 9.591            | 15.056       | 0.044           |
| CD326   | 3.864            | 21.444       | 0.044           |
| CD133/1 | 1.045            | 14.278       | 0.019           |
| CD142   | 1.727            | 15.000       | 0.006           |
| CD45    | 40.318           | 14.167       | 0.019           |
| CD14    | 8.773            | 49.778       | 0.006           |

**TABLE 4 |** Association between baseline markers values and age in BC patients. Spearman correlation was used to perform analysis. If  $r_s$  is positive, age and marker expression are directly/positively proportional; if  $r_s$  is negative, age, and marker expression are negatively correlated.

|       | Age   |                 |
|-------|-------|-----------------|
|       | $r_s$ | <i>p</i> -value |
| CD105 | 0.79  | 0.006           |
| CD1c  | -0.82 | 0.004           |
| CD62p | 0.69  | 0.029           |
| CD41b | 0.72  | 0.019           |
| CD42a | 0.68  | 0.031           |
| CD326 | 0.75  | 0.012           |
| CD29  | 0.68  | 0.031           |

**TABLE 3 |** Summary of significant values calculated through analysis of mean values of plasma EVs derived from BC patients at different time points (before surgical intervention, 1 month after surgical intervention and 6 months after surgical intervention). MFI, mean fluorescence intensity. ANOVA test for repeated measures was used to perform analysis.

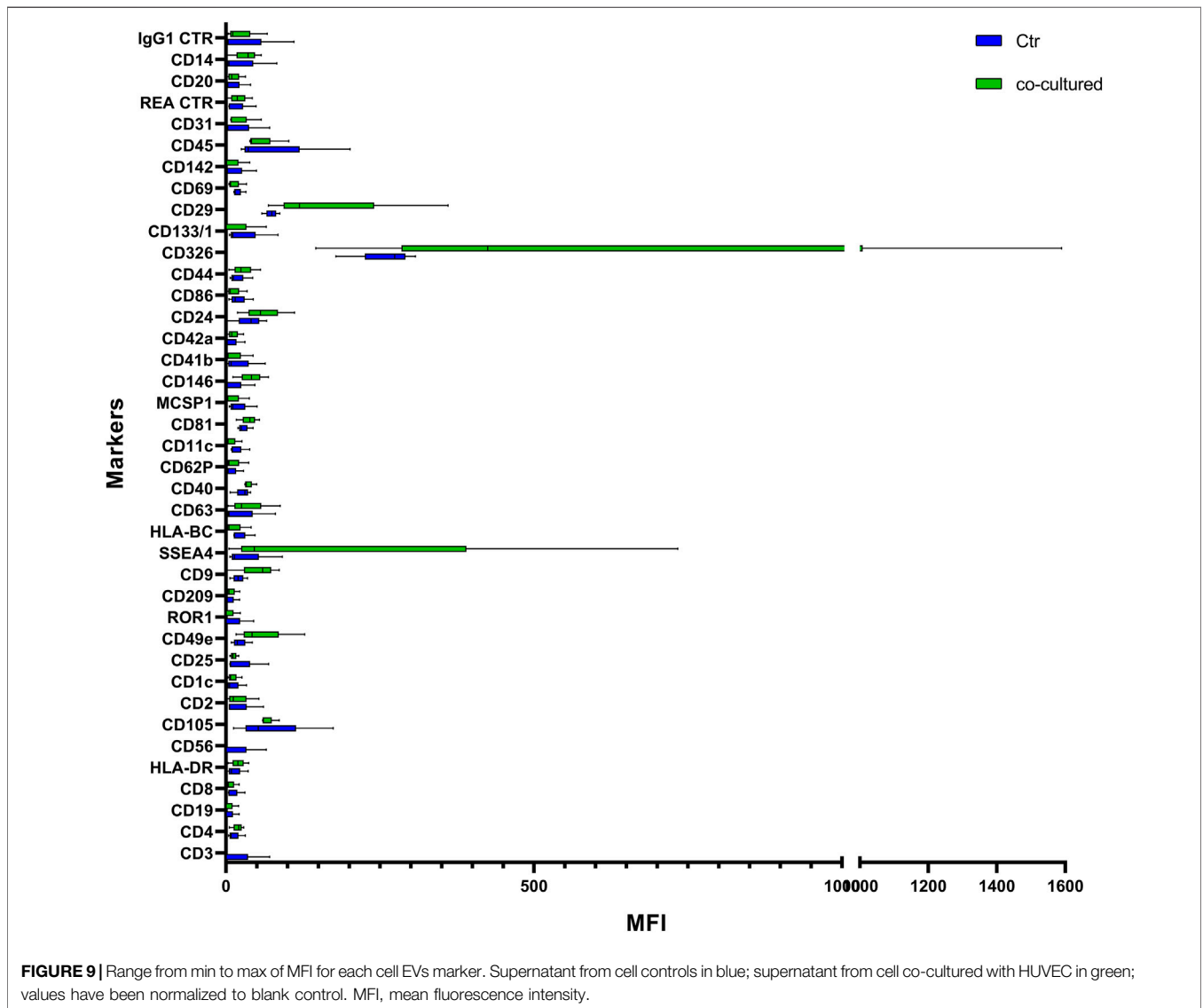
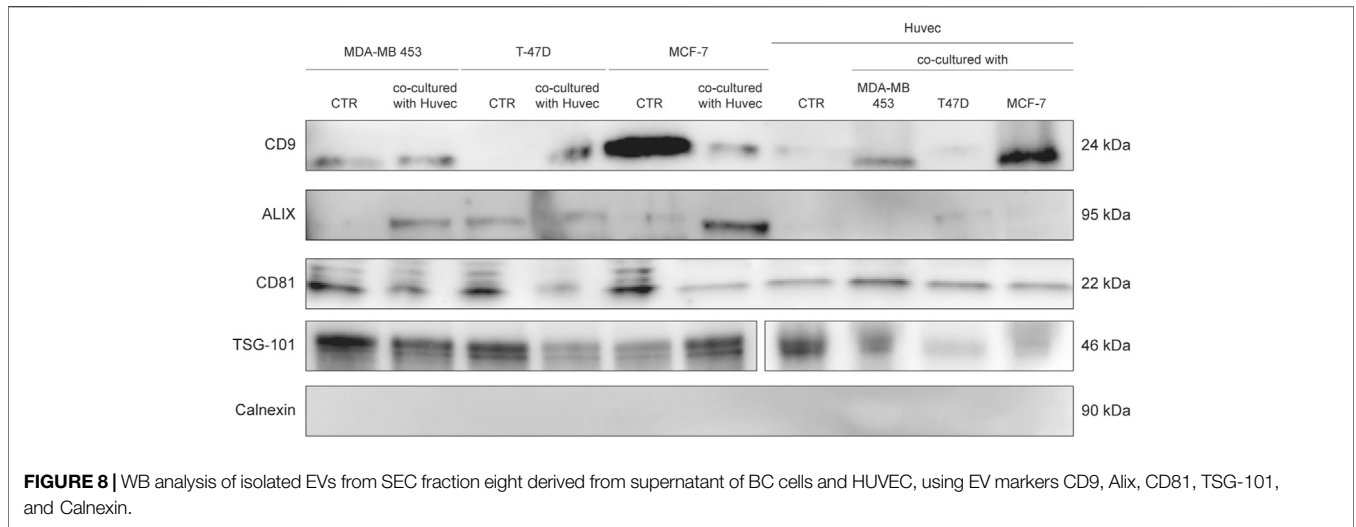
| Markers | Mean MFI time A | Mean MFI time B | Mean MFI time C | <i>p</i> -value |
|---------|-----------------|-----------------|-----------------|-----------------|
| CD146   | 24.444          | 8.722           | 10.111          | 0.034           |
| CD45    | 14.167          | 4.889           | 104.056         | 0.047           |

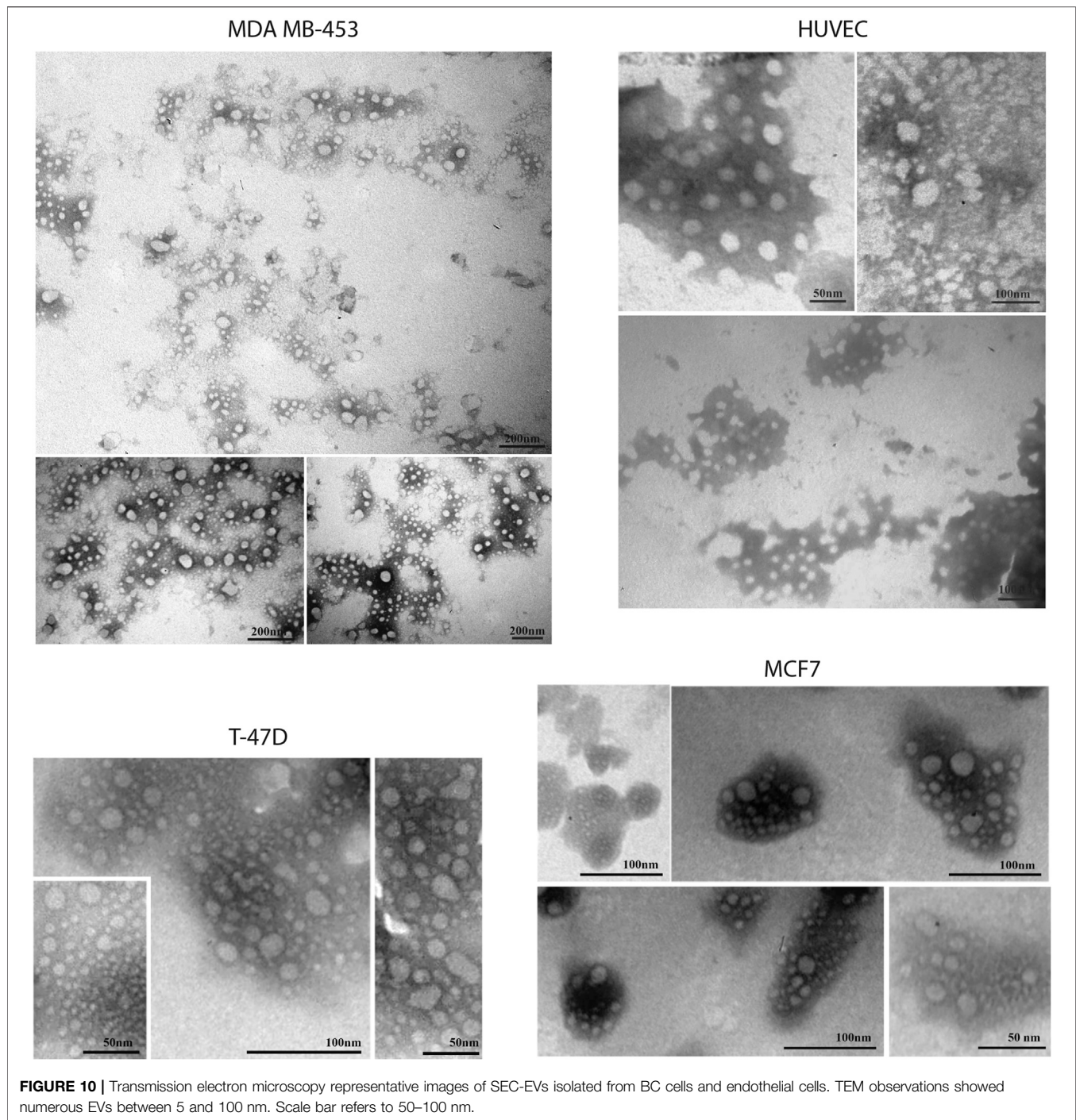


## Characterization of EVs Isolated From BC Cell Lines

EVs were successfully isolated from BC and HUVEC cell lines through SEC. NTA showed a similar distribution for EVs from three different BC cells: MDA-MB 453 EVs had a mean size of 120.5 nm in controls and 120.6 in co-cultured samples; T-47D EVs had a mean size of 123.1 in controls and 118 in co-cultured samples; MCF-7 EVs had a mean size of 131.4 in controls and 123.3 in co-cultured samples. All cell lines showed concentrations between  $4.4 \times 10^{10}$  –  $7 \times 10^{10}$  particles/ml as shown in **Figure 7**. Interestingly, we

observed a slight trend for vesicles to increase their production or release in co-cultured cells compared to the controls, in particular for MDA-MB 453 ( $4.4 \times 10^{10}$  control cells vs.  $5.52 \times 10^{10}$  co-cultured cells) and T-47D ( $5.5 \times 10^{10}$  control cells vs.  $7 \times 10^{10}$  co-cultured cells) cell lines. EVs from HUVEC cells were slightly larger compared to those from BC cells, being characterized by a mean size of 134.9 nm in control cells, and by means varying from 118–131.4 nm when co-cultured with BC cell lines, together with lower concentrations between  $9.36 \times 10^9$  –  $1.7 \times 10^{10}$  particles/ml. No significant differences were observed between control and





co-cultured cells for vesicle size. Western blot analysis showed that EVs of BC cells and HUVEC were positive, at different levels, for CD9, Alix, CD81, and TSG-101, and negative for the expression of Calnexin (**Figure 8**). Furthermore, vesicles were analyzed both by flow cytometry and TEM. Flow cytometry analysis revealed a variation in the expression of exosomal markers between co-cultured cells and controls (**Figure 9**). The morphology of EVs isolated from BC cells was examined through

TEM analysis. MDA-MB 453 were characterized by vesicles with sizes between 20–100 nm and not all of them characterized by well-preserved membranes; T-47D cells were defined by preserved membranes and small vesicles of size between 5–30 nm, some with irregular shape. MCF-7 cells were characterized by preserved membranes and EVs with sizes between 5–25 nm. HUVEC showed less conserved membranes and their vesicles were characterized by a size between 20–60 nm (**Figure 10**).

**TABLE 5 |** Summary of significant values calculated through analysis of mean values of EVs derived from supernatant of BC cell lines and controls. MFI: mean fluorescent intensity; Ctr: control. Two independent experiments were performed and 3 cell lines were used (control groups,  $n = 3$  and co-cultured groups,  $n = 3$ ). Unpaired Student's  $t$  test was used to perform the analysis.

| Markers | Mean MFI Ctr | Mean MFI co-cultured | $p$ -value |
|---------|--------------|----------------------|------------|
| CD4     | 14.833       | 18.500               | 0.025      |
| CD105   | 79.667       | 69.000               | 0.025      |
| CD40    | 26.00        | 38.000               | 0.025      |
| CD146   | 16.333       | 40.667               | 0.025      |
| CD44    | 20.833       | 28.500               | 0.025      |
| CD29    | 73.500       | 183.000              | 0.025      |

## EVs Differentially Expressed in Vesicles Derived From BC Cells After Co-culture With Endothelial Cells

Cytofluorimetric EVs analysis showed six significant antigens discriminating between BC cells co-cultured with ECs and BC cells alone with a  $p$ -value  $< 0.05$ : CD4, CD105, CD40, CD146, CD44, and CD29 (Table 5). CD105 ( $p = 0.001$ ) and CD40 ( $p = 0.006$ ) were further confirmed as factors that clearly distinguished EVs derived from BC cells co-cultured with ECs, along with CD81 as correlated to co-cultured phenotype ( $p = 0.0005$ ).

## DISCUSSION

In BC, clinicopathological characteristics such as age, grade, stage, and molecular subtypes correlate to different incidences, survival, prognosis, and biology, influencing clinical decisions. In addition to tumor cell biology, an inflammatory microenvironment can be responsible for cancer growth. In fact, to date, it is well known that TME can affect carcinogenesis at various steps, from initiation to progression (Tekpli et al., 2019). Many risk factors have been recognized for BC development including age, family history, genetic mutations, chronic inflammation, obesity, and personal habits. Indeed, cancer development is a complex and progressive process that involves modifications not only in the tumor initiating cells, but also in the surrounding environment constituted by several types of cells and secreted biomolecules (Deshmukh et al., 2019), among which EVs are the key of this interplay.

Equally importantly, the interaction between tumor cells and TME at metastatic sites has been recognized as a key regulator of tumor progression, and a better understanding of the mechanisms through which BC-derived EVs guide secondary metastasis is so crucial (Kim et al., 2020).

TME includes a variety of cell types: fibroblasts, ECs, immune cells, pericytes, adipocytes, and local and bone marrow-derived cells, surrounded by matrix components. Moreover, blood supply plays a pivotal role in cancer progression, allowing access to oxygen and nutrients that support tumor spread and eliminate metabolic waste. In this context, angiogenesis, the process by which new blood vessels arise from pre-existing ones, represents a central step in the progression of tumor growth and metastases dissemination, and the blockade of angiogenesis is a promising challenge for new cancer therapies. Hence, although somewhat partial, studying the

possible interaction between ECs and BC cells through *in vitro* studies of EVs could be a fair starting point to solve and more deeply understand the intricate interactions between cancer cells and TME (Bovy et al., 2015). In the future, it should be possible to translate the findings into the clinic after identification of tumor-specific actionable targets and validation of new EV-based markers of prognosis and/or resistance to therapy (Möller and Lobb, 2020).

The release of EVs into the extracellular space means a chance to examine them in body fluids such as blood, urine, liquor, and malignant effusions, making them potential biomarkers for the clinical management of cancer with some notable advantages (Mathew et al., 2020). First of all it is a non-invasive way to recover samples from a number of biologic materials. Secondly, circulating EVs analysis could represent a “liquid biopsy” with the convenience of not requesting cancerous tissue or the partial or total removal of a tumor to access its molecular information, and the capability to monitor cancer progression due to consecutive repeatable sampling (Lucchetti et al., 2019). However, one of the main issues highlighted by the scientific community concerns the absence of a standardized protocol for enrichment and characterization of EVs (Lane et al., 2018), although numerous methods have been developed in order to investigate their behavior. Generally, EVs can be differentiated by size, density, and protein composition, but it is still demanding to easily fractionate EVs and microvesicles due to the marked similarity of their composition. EVs can be isolated through a variety of techniques, such as centrifugation (high speed, differential, and density-gradient), membrane affinity columns, SEC, filtration, and precipitation. Many of these methods are characterized by poor purity and consistence (Hu T. et al., 2021). Besides the most commonly used approaches to obtain EVs, which have some limitations (Greening et al., 2015; Lobb et al., 2015), several other strategies, including flow cytometry ones, are gaining interest (Maia et al., 2020; Marchisio et al., 2020). Hence, before translating into clinics, methods such as that herein reported (Salvi et al., 2021) need to be tested, and clinical validations need to be performed. In order to investigate blood-related TME and discover new potential disease-related biomarkers through a recent approach, we performed a small case study, highlighting the feasibility of the detection and characterization of BC-derived EVs. We used both plasma samples of BC patients and BC cell lines co-cultured with ECs. Patient samples were taken before surgery, and after 1 and 6 months after surgery, together with adjuvant therapy, to investigate the value of EVs as cancer markers in this clinical setting during the earliest stage of the disease, in order to discover possible biomarkers to monitor patients in the first months after surgery and/or during therapy. We first isolated EVs through SEC, and then characterized EVs through NTA, WB, and a multiplexed phenotyping cytofluorimetric approach able to detect 37 exosomes-related antigens. NTA analysis of EVs derived from BC patients did not show a variation in the dimensions of vesicles compared to that of healthy subjects, but significant results were observed among the three different time points, especially in vesicles analyzed 1 month post-surgery. The MACSPlex-based characterization showed that CD3, CD56, CD2, CD25, CD9, CD44, CD326, CD133/

1, CD142, CD45, and CD14 markers were differentially expressed, with significance, between healthy subjects and patients. Interestingly, CD146 and CD45 were found significantly deregulated at the three different time points. In particular, both CD146 and CD45 expression levels were reduced in EVs 1 month after surgical resection, suggesting that these markers could have a value for monitoring disease after surgical resection, therapy, and progression. In line with these results, CD146 is considered a hallmark of tumor progression and metastasis, especially in TNBC (Li et al., 2021) and CD45 was found deregulated in breast stroma of BC patients at early stages also (Marino et al., 2020). Furthermore, CD146 is a well-known endothelial cell lineage marker. Firstly identified as a melanoma cell adhesion molecule (MCAM), it is overexpressed in many tumors and implicated in vascular and lymphatic metastasis (Wang et al., 2020). CD146 is a molecule known to modulate cell-cell adhesion and to bind to extracellular matrix proteins or other transmembrane proteins, such as VEGFR2, and the secretion of CD146-enriched EVs was reported to be associated with metastatic process, mediating their interaction with specific ligands on endothelial cells of metastatic organs (Ghoroghi et al., 2021). Since we observed a CD146 decrease during the time in which patients did not progress in 5 years, it is tempting to hypothesize that a reduction of this marker could be related to a better prognosis. We further reported deregulated markers whose presence suggests a peculiar asset of EVs in aging cancer patients. Specific age-related EV markers is a field that would be worth being studied, in particular to more deeply understand the well-known association between cancer and aging.

In order to shed some light on the EV epitopes we found in the clinical setting, we set up an experimental plan *in vitro* that could confirm the results obtained for deregulated markers observed. In our cell models, the interaction of BC cells with ECs firstly seems to lead to a slight increase of EV release, compared to the number of EVs produced by cancer or HUVEC cells. A range of markers were identified with increased signal intensity in samples co-cultured with ECs: CD4, CD105, CD40, CD146, CD44, CD29, and CD81, with only CD44 and CD146 variation found common in both patients and cell models. Although results between BC cells and patients were not completely comparable, most probably due to the different nature of samples, the increase of these markers in BC cells-released vesicles may hint some interesting thoughts. The interaction of cancer cells with a simplified normal microenvironment (herein streamlined by HUVEC cells) may trigger the production of EVs exhibiting antigens related to endothelial/neo-angiogenetic and/or aggressiveness features. Indeed, CD146 and CD44 have been related to neo-angiogenesis, cell proliferation, cell survival, cytoskeletal changes, and cellular motility (Chen et al., 2018). This may suggest an involvement of ECs in the acquisition of a more aggressive behavior of cancer cells, as already reported (Hwang et al., 2020). Despite not being significantly different in BC patients vs healthy donors, CD146 expression decreased in our BC patients over time, as previously reported here, suggesting a role in tumor related neo-angiogenetic processes. On the other hand, CD44 was altered both in patients vs healthy subjects and in cell models, suggesting that this could be a cancer-related marker

of spreading and prompting a deeper investigation of this antigen in BC patient EVs. Furthermore, a recent study showed that CD44 circulating tumor endothelial cells were associated with poor prognosis in pancreatic ductal adenocarcinoma after radical surgery (Xing et al., 2021). Indeed, the identification of circulating factors that might be responsible for influencing and spreading vessels formation, modulating angiogenesis and aggressiveness, it is of great clinical interest. It is increasingly necessary to support the study of new biomarkers of angiogenesis and metastatic spread, with the final aim of an accurate disease monitoring targeted towards personalized medicine. In agreement, a study reported a high percentage of patients exhibiting high tumor-infiltrating lymphocytes with CD3 positivity exhibited pathological response to neoadjuvant chemotherapy (Gomez-Macias et al., 2020). From this point of view, in the future, the herein feasible detection of CD3-positive EVs, potentially secreted by CD-positive infiltrating lymphocytes, could also be investigated and utilized as a marker of response. In summary, we performed a small preliminary and feasibility study to investigate useful biomarkers possibly exploitable for diagnostic and monitoring intent, as already reported for monitoring therapies in various types of cancer (Stevic et al., 2020). Moreover, although dissimilar from the clinical setting in terms of expression of some markers, the results from *in vitro* analysis of EVs suggested the implication of CD44 and CD146 in biological processes involved in breast tumor and microenvironment interplay. The fact that we observed significant results already in a small but well monitored series of patients recommends continuing in this direction. However, since we are aware of the limitations of this study, principally due to the small size of our patient cohort, future validation studies with a larger set of patients are clearly needed.

## DATA AVAILABILITY STATEMENT

The raw data supporting the conclusions of this article will be made available by the authors, without undue reservation.

## ETHICS STATEMENT

The studies involving human participants were reviewed and approved by the Romagna Ethics Committee (CEROM) of Meldola IRCCS IRST (IRSTB008). The patients/participants provided their written informed consents to participate in this study.

## AUTHOR CONTRIBUTIONS

EB and TR constructed this study. EB, TR, IV, MM, SSalu, MB, and FF performed the experiments. ES and IA performed the formal data analysis. RM and PS were responsible for clinical resources. GG, SSalu, and WCC performed data curation and interpretation. FF was responsible for the supervision of the project. All authors contributed to the article and approved the submitted version.

## FUNDING

TR was supported as Fellows by the Associazione Annastaccatolisa ONLUS (Montecatini Terme, Pistoia, Italy) research scholar funds.

## REFERENCES

- Bandini, E., and Fanini, F. (2019). MicroRNAs and Androgen Receptor: Emerging Players in Breast Cancer. *Front. Genet.* 10, 203. doi:10.3389/fgene.2019.00203
- Barone, I., Giordano, C., Bonofiglio, D., Andò, S., and Catalano, S. (2020). The Weight of Obesity in Breast Cancer Progression and Metastasis: Clinical and Molecular Perspectives. *Semin. Cancer Biol.* 60, 274–284. doi:10.1016/j.semcancer.2019.09.001
- Bovy, N., Blomme, B., Frères, P., Dederen, S., Nivelles, O., Lion, M., et al. (2015). Endothelial Exosomes Contribute to the Antitumor Response during Breast Cancer Neoadjuvant Chemotherapy via microRNA Transfer. *Oncotarget* 6, 10253–10266. doi:10.18632/oncotarget.3520
- Brahmer, A., Neuberger, E., Esch-Heisser, L., Haller, N., Jorgensen, M. M., Baek, R., et al. (2019). Platelets, Endothelial Cells and Leukocytes Contribute to the Exercise-Triggered Release of Extracellular Vesicles into the Circulation. *J. Extracell. Vesicles* 8, 1615820. doi:10.1080/20013078.2019.1615820
- Burgio, S., Noori, L., Marino Gammazza, A., Campanella, C., Logozzi, M., Fais, S., et al. (2020). Extracellular Vesicles-Based Drug Delivery Systems: A New Challenge and the Exemplum of Malignant Pleural Mesothelioma. *Int. J. Mol. Sci.* 21, 5432. doi:10.3390/ijms21155432
- Chan, J. C. H., Chow, J. C. H., Ho, C. H. M., Tsui, T. Y. M., and Cho, W. C. (2021). Clinical Application of Circulating Tumor DNA in Breast Cancer. *J. Cancer Res. Clin. Oncol.* 147 (5), 1431–1442. doi:10.1007/s00432-021-03588-5
- Chen, C., Zhao, S., Karnad, A., and Freeman, J. W. (2018). The Biology and Role of CD44 in Cancer Progression: Therapeutic Implications. *J. Hematol. Oncol.* 11, 64. doi:10.1186/s13045-018-0605-5
- Chen, W.-Z., Jiang, J.-X., Yu, X.-Y., Xia, W.-J., Yu, P.-X., Wang, K., et al. (2019). Endothelial Cells in Colorectal Cancer. *World J. Gastrointest. Oncol.* 11, 946–956. doi:10.4251/wjgo.v11.i11.946
- Deshmukh, S. K., Srivastava, S. K., Poosarla, T., Dyess, D. L., Holliday, N. P., Singh, A. P., et al. (2019). Inflammation, Immunosuppressive Microenvironment and Breast Cancer: Opportunities for Cancer Prevention and Therapy. *Ann. Transl. Med.* 7, 593. doi:10.21037/atm.2019.09.68
- Devadas, D., Moore, T. A., Walji, N., and Young, E. W. K. (2019). A Microfluidic Mammary Gland Coculture Model Using Parallel 3D Lumens for Studying Epithelial-Endothelial Migration in Breast Cancer. *Biomicrofluidics* 13, 064122. doi:10.1063/1.5123912
- Draoui, N., de Zeeuw, P., and Carmeliet, P. (2017). Angiogenesis Revisited from a Metabolic Perspective: Role and Therapeutic Implications of Endothelial Cell Metabolism. *Open Biol.* 7, 170219. doi:10.1098/rsob.170219
- Ghoroghi, S., Mary, B., Larnicol, A., Asokan, N., Klein, A., Osmani, N., et al. (2021). Ral GTPases Promote Breast Cancer Metastasis by Controlling Biogenesis and Organ Targeting of Exosomes. *Elife* 10, e61539. doi:10.7554/eLife.61539
- Gomez-Macias, G., Molinar-Flores, G., Lopez-Garcia, C., Santuario-Facio, S., Decanini-Arcaute, H., Valero-Elizondo, J., et al. (2020). Immunotyping of Tumor Infiltrating Lymphocytes in Triple Negative Breast Cancer and Genetic Characterization. *Oncol. Lett.* 20, 1. doi:10.3892/ol.2020.12000
- Greening, D. W., Xu, R., Ji, H., Tauro, B. J., and Simpson, R. J. (2015). "A Protocol for Exosome Isolation and Characterization: Evaluation of Ultracentrifugation, Density-Gradient Separation, and Immunoaffinity Capture Methods, 1295. 179, 209. doi:10.1007/978-1-4939-2550-6\_15
- Hoshino, I. (2021). The Usefulness of microRNA in Urine and Saliva as a Biomarker of Gastroenterological Cancer. *Int. J. Clin. Oncol.* 26, 1431–1440. doi:10.1007/s10147-021-01911-1
- Hu, H., Ling, B., Shi, Y., Wu, H., Zhu, B., Meng, Y., et al. (2021a). Plasma Exosome-Derived SENP1 May Be a Potential Prognostic Predictor for Melanoma. *Front. Oncol.* 11, 685009. doi:10.3389/fonc.2021.685009
- Hu, T., Wolfram, J., and Srivastava, S. (2021b). Extracellular Vesicles in Cancer Detection: Hopes and Hypes. *Trends Cancer* 7, 122–133. doi:10.1016/j.trecan.2020.09.003
- Hwang, H. J., Lee, Y.-R., Kang, D., Lee, H. C., Seo, H. R., Ryu, J.-K., et al. (2020). Endothelial Cells under Therapy-Induced Senescence Secrete CXCL11, Which Increases Aggressiveness of Breast Cancer Cells. *Cancer Lett.* 490, 100–110. doi:10.1016/j.canlet.2020.06.019
- Jayaseelan, V. P. (2020). Emerging Role of Exosomes as Promising Diagnostic Tool for Cancer. *Cancer Gene Ther.* 27, 395–398. doi:10.1038/s41417-019-0136-4
- Jong, A. Y., Wu, C.-H., Li, J., Sun, J., Fabbri, M., Wayne, A. S., et al. (2017). Large-scale Isolation and Cytotoxicity of Extracellular Vesicles Derived from Activated Human Natural Killer Cells. *J. Extracell. Vesicles* 6, 1294368. doi:10.1080/20013078.2017.1294368
- Kim, J., Lee, C., Kim, I., Ro, J., Kim, J., Min, Y., et al. (2020). Three-Dimensional Human Liver-Chip Emulating Premetastatic Niche Formation by Breast Cancer-Derived Extracellular Vesicles. *ACS Nano* 14, 14971–14988. doi:10.1021/acsnano.0c04778
- Kourti, M., Cai, J., Jiang, W., and Westwell, A. D. (2020). Structural Modifications on CORM-3 Lead to Enhanced Anti-angiogenic Properties against Triple-Negative Breast Cancer Cells. *Med. Chem.* 17, 40–59. doi:10.2174/1573406415666191206102452
- Lane, R. E., Korbie, D., Hill, M. M., and Trau, M. (2018). Extracellular Vesicles as Circulating Cancer Biomarkers: Opportunities and Challenges. *Clin. Transl. Med.* 7, 14. doi:10.1186/s40169-018-0192-7
- Li, C., Kang, L., Fan, K., Ferreira, C. A., Becker, K. V., Huo, N., et al. (2021). ImmunoPET of CD146 in Orthotopic and Metastatic Breast Cancer Models. *Bioconjug. Chem.* 32, 1306–1314. doi:10.1021/acs.bioconjchem.0c00649
- Lobb, R. J., Becker, M., Wen Wen, S., Wong, C. S. F., Wiegman, A. P., Leimgruber, A., et al. (2015). Optimized Exosome Isolation Protocol for Cell Culture Supernatant and Human Plasma. *J. Extracell. Vesicles* 4, 27031. doi:10.3402/jev.v4.27031
- López-Pérez, Ó., Sanz-Rubio, D., Hernaiz, A., Betancor, M., Otero, A., Castilla, J., et al. (2021). Cerebrospinal Fluid and Plasma Small Extracellular Vesicles and miRNAs as Biomarkers for Prion Diseases. *Int. J. Mol. Sci.* 22, 6822. doi:10.3390/ijms22136822
- Lucchetti, D., Fattorossi, A., and Sgambato, A. (2019). Extracellular Vesicles in Oncology: Progress and Pitfalls in the Methods of Isolation and Analysis. *Biotechnol. J.* 14, 1700716. doi:10.1002/biot.201700716
- Madden, E. C., Gorman, A. M., Logue, S. E., and Samali, A. (2020). Tumour Cell Secretome in Chemoresistance and Tumour Recurrence. *Trends Cancer* 6, 489–505. doi:10.1016/j.trecan.2020.02.020
- Maia, J., Batista, S., Couto, N., Gregório, A. C., Bodo, C., Elzanowska, J., et al. (2020). Employing Flow Cytometry to Extracellular Vesicles Sample Microvolume Analysis and Quality Control. *Front. Cel. Dev. Biol.* 8, 593750. doi:10.3389/fcell.2020.593750
- Malvezzi, M., Carioli, G., Bertuccio, P., Boffetta, P., Levi, F., La Vecchia, C., et al. (2019). European Cancer Mortality Predictions for the Year 2019 with Focus on Breast Cancer. *Ann. Oncol.* 30, 781–787. doi:10.1093/annonc/mdz051
- Marchisio, M., Simeone, P., Bologna, G., Ercolino, E., Pierdomenico, L., Pieragostino, D., et al. (2020). Flow Cytometry Analysis of Circulating Extracellular Vesicle Subtypes from Fresh Peripheral Blood Samples. *Int. J. Mol. Sci.* 22, 48. doi:10.3390/ijms22010048

## SUPPLEMENTARY MATERIAL

The Supplementary Material for this article can be found online at: <https://www.frontiersin.org/articles/10.3389/fmolb.2021.732900/full#supplementary-material>

- Marino, N., German, R., Rao, X., Simpson, E., Liu, S., Wan, J., et al. (2020). Upregulation of Lipid Metabolism Genes in the Breast Prior to Cancer Diagnosis. *npj Breast Cancer* 6, 50. doi:10.1038/s41523-020-00191-8
- Mathew, M., Zade, M., Mezghani, N., Patel, R., Wang, Y., and Momen-Heravi, F. (2020). Extracellular Vesicles as Biomarkers in Cancer Immunotherapy. *Cancers* 12, 2825. doi:10.3390/cancers12102825
- Möller, A., and Lobb, R. J. (2020). The Evolving Translational Potential of Small Extracellular Vesicles in Cancer. *Nat. Rev. Cancer* 20, 697–709. doi:10.1038/s41568-020-00299-w
- Romano, R., Picca, A., Eusebi, L. H. U., Marzetti, E., Calvani, R., Moro, L., et al. (2021). Extracellular Vesicles and Pancreatic Cancer: Insights on the Roles of miRNA, lncRNA, and Protein Cargos in Cancer Progression. *Cells* 10, 1361. doi:10.3390/cells10061361
- Salvi, S., Bandini, E., Carloni, S., Casadio, V., Battistelli, M., Salucci, S., et al. (2021). Detection and Investigation of Extracellular Vesicles in Serum and Urine Supernatant of Prostate Cancer Patients. *Diagnostics* 11, 466. doi:10.3390/diagnostics11030466
- Sempere, L., Keto, J., and Fabbri, M. (2017). Exosomal MicroRNAs in Breast Cancer towards Diagnostic and Therapeutic Applications. *Cancers* 9, 71. doi:10.3390/cancers9070071
- Shah, K. B., Chernausk, S. D., Garman, L. D., Pezant, N. P., Plows, J. F., Kharoud, H. K., et al. (2021). Human Milk Exosomal MicroRNA: Associations with Maternal Overweight/Obesity and Infant Body Composition at 1 Month of Life. *Nutrients* 13, 1091. doi:10.3390/nu13041091
- Singletary, S. E., and Connolly, J. L. (2006). Breast Cancer Staging: Working with the Sixth Edition of the AJCC Cancer Staging Manual. *CA: A Cancer J. Clin.* 56, 37–47. doi:10.3322/canjclin.56.1.37
- Stevic, I., Buescher, G., and Ricklefs, F. L. (2020). Monitoring Therapy Efficiency in Cancer through Extracellular Vesicles. *Cells* 9, 130. doi:10.3390/cells9010130
- Sung, H., Ferlay, J., Siegel, R. L., Laversanne, M., Soerjomataram, I., Jemal, A., et al. (2021). Global Cancer Statistics 2020: GLOBOCAN Estimates of Incidence and Mortality Worldwide for 36 Cancers in 185 Countries. *CA A. Cancer J. Clin.* 71, 209–249. doi:10.3322/caac.21660
- Tekpli, X., Lien, T., Lien, T., Rossevoid, A. H., Nebdal, D., Borgen, E., et al. (2019). An Independent Poor-Prognosis Subtype of Breast Cancer Defined by a Distinct Tumor Immune Microenvironment. *Nat. Commun.* 10, 5499. doi:10.1038/s41467-019-13329-5
- Wang, Z., Xu, Q., Zhang, N., Du, X., Xu, G., and Yan, X. (2020). CD146, from a Melanoma Cell Adhesion Molecule to a Signaling Receptor. *Sig. Transduct. Target. Ther.* 5, 148. doi:10.1038/s41392-020-00259-8
- Wu, C.-H., Li, J., Li, L., Sun, J., Fabbri, M., Wayne, A. S., et al. (2019). Extracellular Vesicles Derived from Natural Killer Cells Use Multiple Cytotoxic Proteins and Killing Mechanisms to Target Cancer Cells. *J. Extracell. Vesicles* 8, 1588538. doi:10.1080/20013078.2019.1588538
- Xing, C., Li, Y., Ding, C., Wang, S., Zhang, H., Chen, L., et al. (2021). CD44+ Circulating Tumor Endothelial Cells Indicate Poor Prognosis in Pancreatic Ductal Adenocarcinoma after Radical Surgery: A Pilot Study. *Cancer Manag. Res.* 13, 4417–4431. doi:10.2147/CMAR.S309115
- Xue, V. W., Yang, C., Wong, S. C. C., and Cho, W. C. S. (2021). Proteomic Profiling in Extracellular Vesicles for Cancer Detection and Monitoring. *Proteomics* 21, 2000094. doi:10.1002/pmic.202000094

**Conflict of Interest:** The authors declare that the research was conducted in the absence of any commercial or financial relationships that could be construed as a potential conflict of interest.

**Publisher's Note:** All claims expressed in this article are solely those of the authors and do not necessarily represent those of their affiliated organizations, or those of the publisher, the editors and the reviewers. Any product that may be evaluated in this article, or claim that may be made by its manufacturer, is not guaranteed or endorsed by the publisher.

Copyright © 2021 Bandini, Rossi, Scarpi, Gallerani, Vannini, Salvi, Azzali, Melloni, Salucci, Battistelli, Serra, Maltoni, Cho and Fabbri. This is an open-access article distributed under the terms of the Creative Commons Attribution License (CC BY). The use, distribution or reproduction in other forums is permitted, provided the original author(s) and the copyright owner(s) are credited and that the original publication in this journal is cited, in accordance with accepted academic practice. No use, distribution or reproduction is permitted which does not comply with these terms.